

Figure S1. Characterization of Fibroblasts and iPSCs, Related to Figure 1

(A) Quantification of immunocytochemical analysis of markers that demonstrate age-associated changes in fibroblasts from donors of different ages. Young: all age 11, middle: ages 31-55, old: ages 71-82, HGPS (Hutchinson-Gilford progeria syndrome): ages 3-14. $n= 3$ independent donors per age group. See Table S1 for additional fibroblast line information.

(B) Quantitative RT-PCR analysis for each *LMNA* isoform in young donor (age 11), old donor (age 82) and HGPS patient (age 14) fibroblasts. Data are presented as mean \pm SEM. $n=3$ consecutive passages.

(C) Reprogramming timeline. HGPS patient fibroblasts required rapamycin treatment to increase progerin turnover and thus reduce the negative effects of progerin-induced phenotypes (Cao et al., 2011) on reprogramming efficiency. OSKM, OCT4/SOX2/KLF4/c-MYC; MEF, mouse embryonic fibroblasts; VPA, valproic acid.

(D) Two representative iPSC clones demonstrated expression of the pluripotency markers NANOG and OCT4 similar to H9 human embryonic stem cells (hESCs) as well as no signs of residual Sendai expression by passage 10.

(E) Flow cytometry analysis of iPSCs for pluripotent (SSEA4, *top*) and fibroblast (HLA-ABC, *bottom*) surface markers. Two representative iPSC clones per donor as well as the donor fibroblasts were compared to H9 hESCs.

(F) Spontaneous differentiation of iPSC clones into three-dimensional embryoid body (EB) structures demonstrates the potential for iPSC clones to upregulate markers of the three germ layers (endoderm: GATA4, AFP; mesoderm: RUNX1, BRACHYURY; ectoderm: NESTIN, NCAM). Images depict representative EBs derived from a single iPSC clone.

(G) Sequencing results show maintenance of the 1824C>T heterozygous mutation through reprogramming in HGPS iPSCs, which was not present in apparently healthy young and old donor-derived fibroblasts or iPSCs.

n.s. not significant, * $p<0.05$, ** $p<0.01$, *** $p<0.001$ according to ANOVA with Dunnett's tests for multiple comparisons. Bar graphs represent mean \pm SEM. Scale bars: 200 μm .

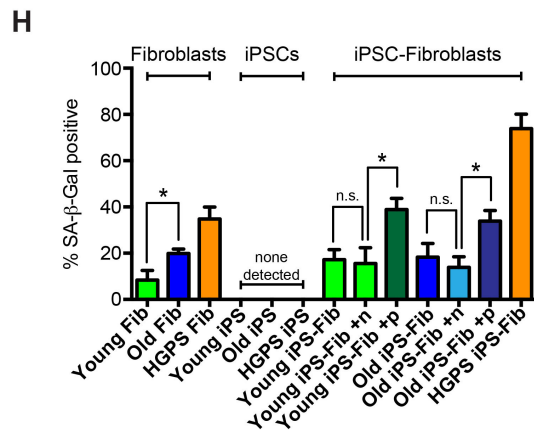
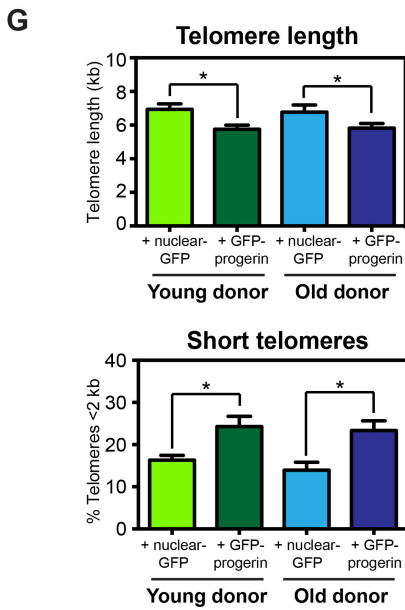
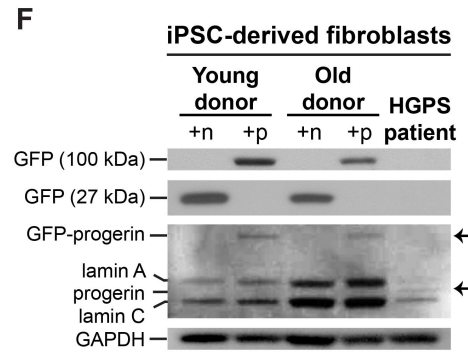
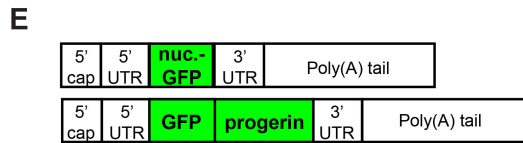
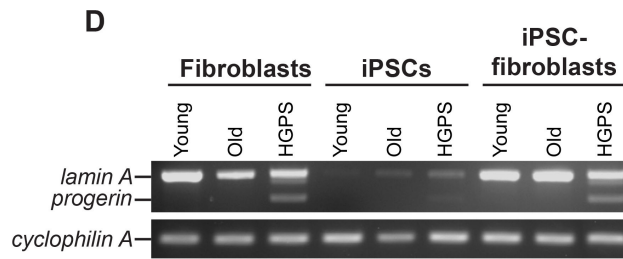
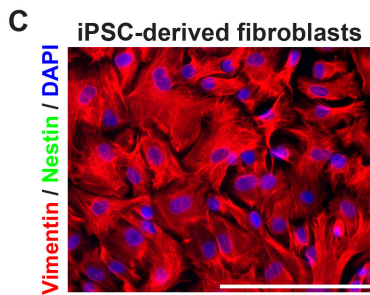
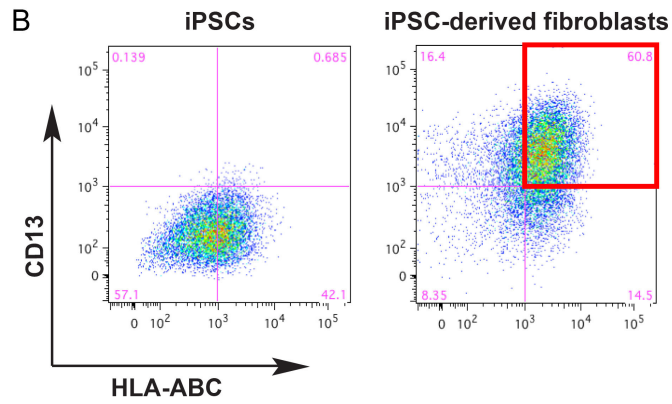
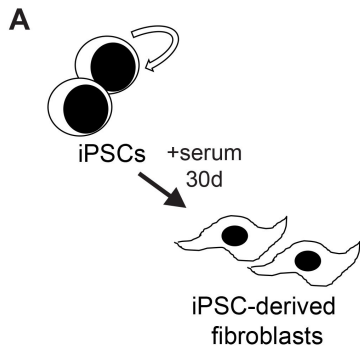


Figure S2. Differentiation of iPSCs to Fibroblast-Like Cells and Overexpression of Progerin Using Modified-RNA, Related to Figures 2 and 3

(A and B) iPSCs were differentiated to fibroblast-like cells in serum-containing medium for 30 days (A) and sorted by flow cytometry (B) for high levels of expression of the fibroblast markers CD13 and HLA-ABC (*red box*) as compared to iPSCs.

(C) iPSC-derived fibroblasts after sorting displayed fibroblast-like morphologies and expression of vimentin but no nestin (a neural marker) by immunocytochemistry.

(D) RT-PCR for *lamin A* and *progerin* transcripts showed upregulation in iPSC-derived fibroblasts (iPSC-fibroblasts) to similar levels observed in the donor fibroblasts.

(E) Modified-RNA was designed to express either nuclear-localized green fluorescent protein (nuclear-GFP) as a control or progerin fused to GFP (GFP-progerin). The addition of generic 5' and 3' UTRs as well as a Poly(A) tail and 5' cap structure facilitated the *in vitro* transcription reaction (Mandal and Rossi, 2013; Warren et al., 2010).

(F) Western blot analysis of transgene expression. n, nuclear-GFP; p, GFP-progerin. Analysis of detection using a lamin A/C antibody (N-18) revealed that progerin overexpression induces levels higher than the endogenous progerin level observed in HGPS iPSC-derived fibroblasts (*arrows*).

(G) Quantification of telomere length and the percentage of telomeres less than 2 kilobases (kb) by Q-FISH. *n*= 4 replicate wells.

(H) Assessment of the senescence markers senescence-activated beta-galactosidase (SA- β -Gal) at all stages from the primary fibroblasts to iPSC-derived fibroblasts overexpressing progerin. *n*= 2 replicate wells.

n.s. not significant, **p*<0.05 according to Student's t-tests. Bar graphs represent mean \pm SEM. Scale bar: 200 μ m.

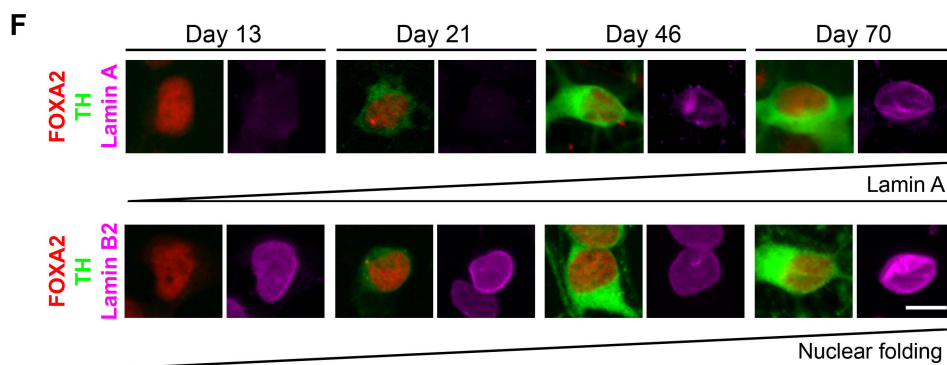
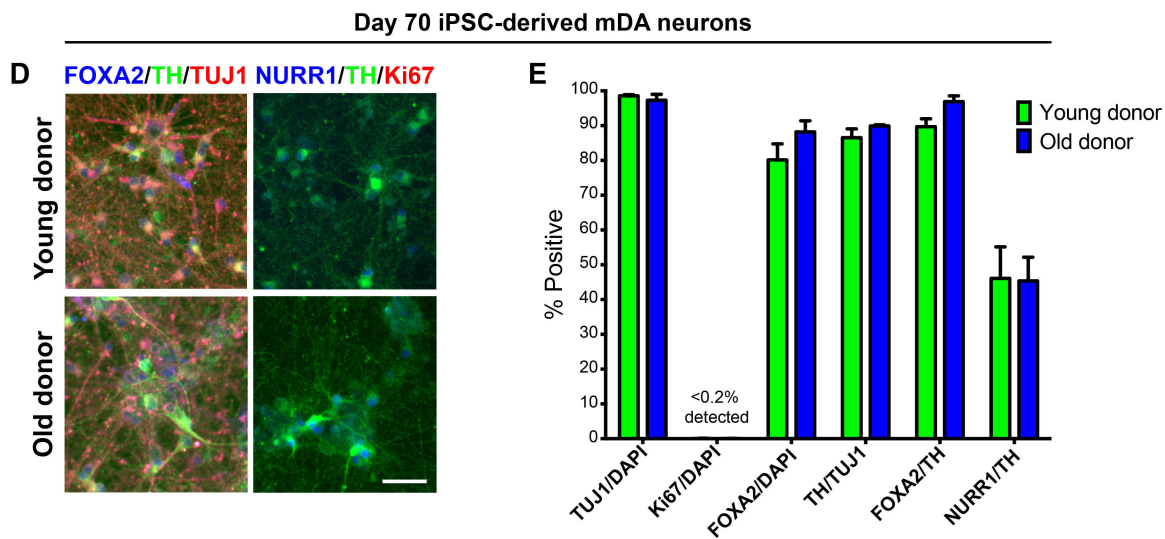
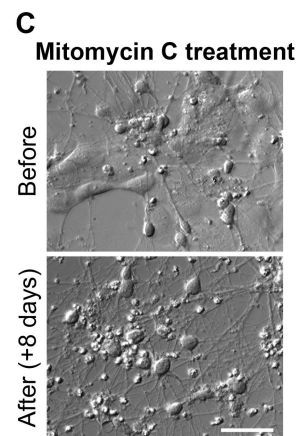
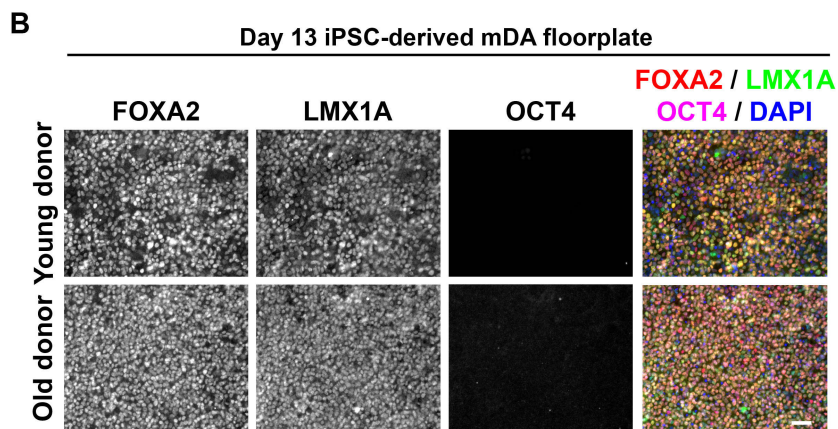
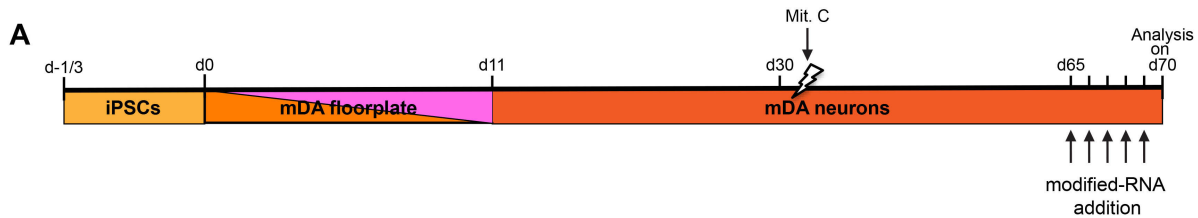


Figure S3. Differentiation of iPSCs to mDA Neurons, Related to Figure 4

(A) Schematic illustration of the differentiation protocol for the derivation of mDA neurons from iPSCs. Mit. C, mitomycin C.

(B) Immunocytochemistry at day 13 of differentiation for FOXA2 (red), LMX1A (green) and OCT4 (pink).

(C) Mitomycin C treatment 1 day following the final day 30 replating helped to eliminate the remaining proliferating cells (post-mitotic neurons unaffected).

(D and E) Immunocytochemistry (D) and quantification (E) demonstrate that almost 100% of the remaining cells at day 70 of differentiation were post-mitotic neurons (TUJ1+/Ki67-) and that greater than 80% of those neurons expressed mDA-specific markers (FOXA2+/TH+). As previously reported (Kriks et al., 2011) approximately 40% of the TH+ neurons also express the more mature mDA marker NURR1. *n*= at least 3 independent differentiations of independent iPSC clones.

(F) Immunocytochemistry for lamin A and lamin B2 during the mDA neuron differentiation shows endogenous upregulation of the lamin A isoform with similar timing to the onset of nuclear folding.

Bar graph represents mean \pm SEM. Scale bars: 50 μ m.

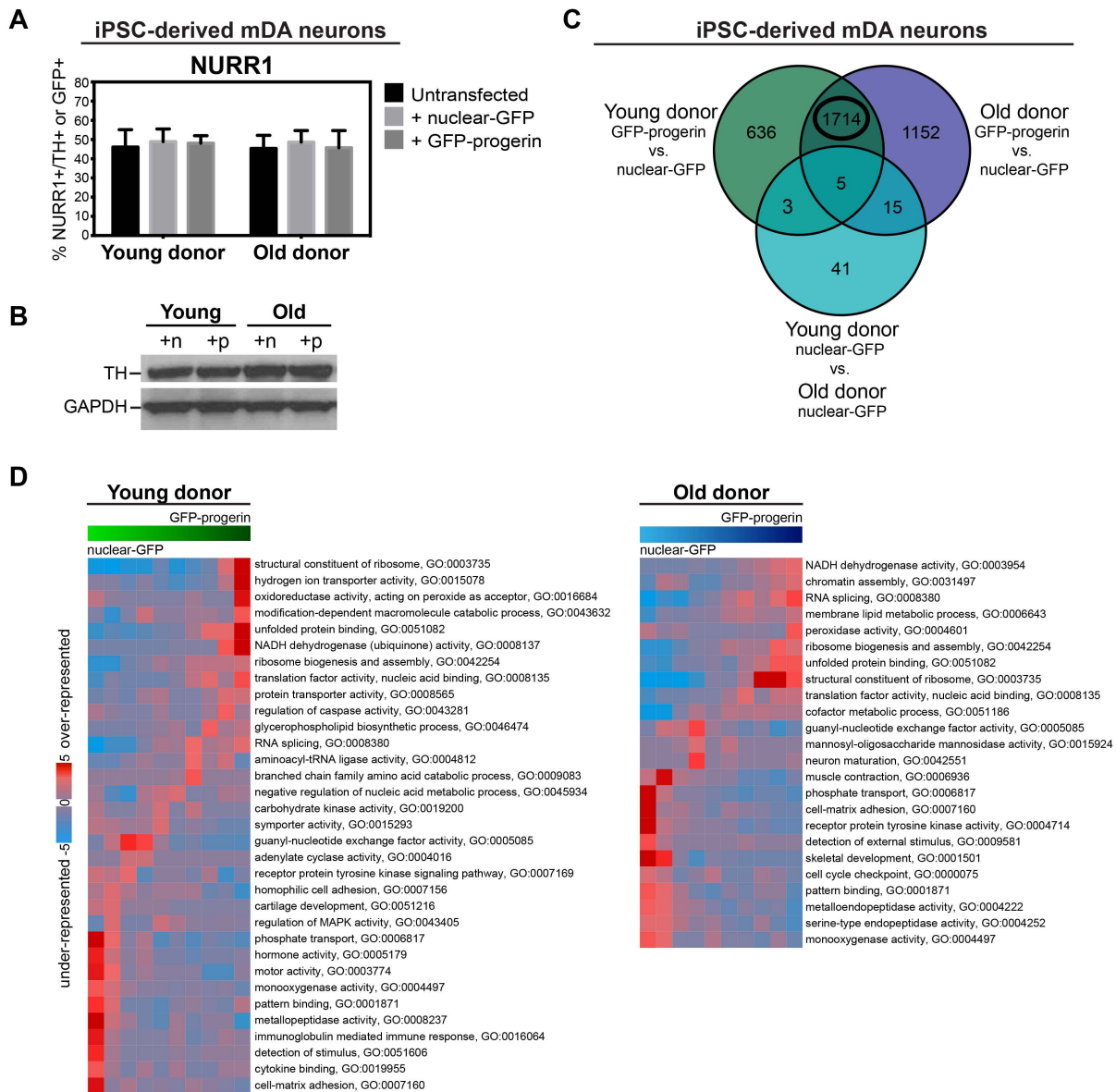


Figure S4. Progerin Overexpression Induces a Neurodegeneration-Like Phenotype, Related to Figure 5

(A and B) The percentage of NURR1+ iPSC-derived mDA neurons (A) and the protein expression levels of TH (B) remained unchanged with transfection, indicating that progerin overexpression does not downregulate key mDA neuron proteins (a typical sign of acute toxicity).

(C) Venn diagram where each colored circle indicates the number of differentially expressed genes (Fold change ± 2 , $p < 0.05$) between two groups. The black circle indicates the overlapping “aging signature” that was further analyzed.

(D) The significant gene ontology terms that are enriched in nuclear-GFP-treated or GFP-progerin-treated iPSC-derived mDA neurons (left to right).

Bar graph represents mean \pm SEM.

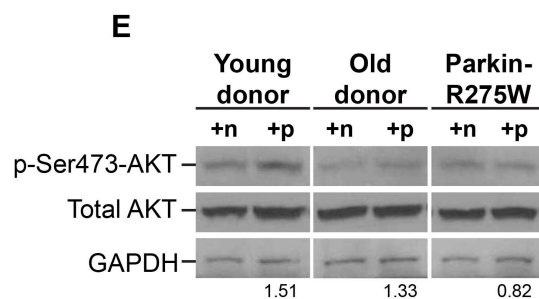
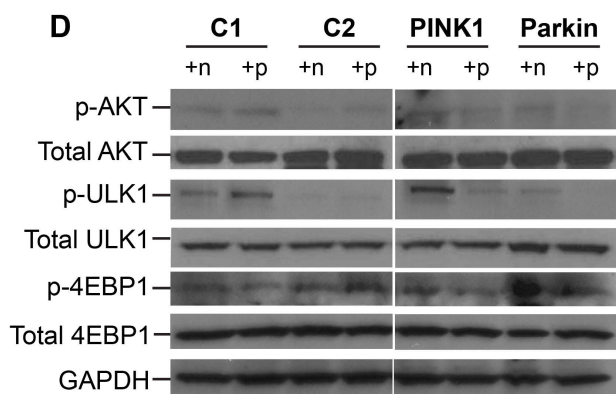
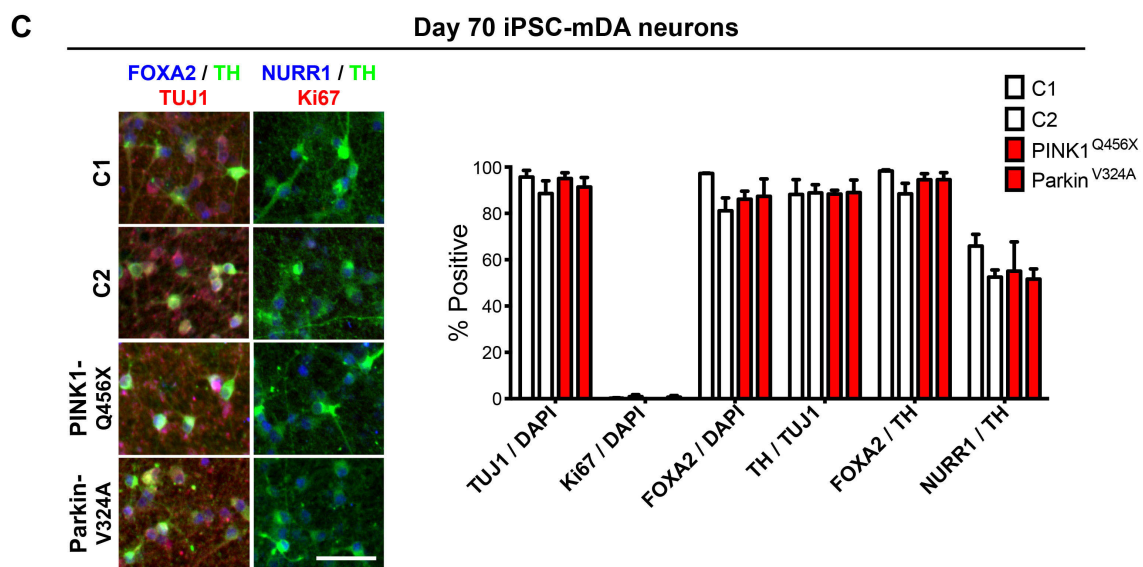
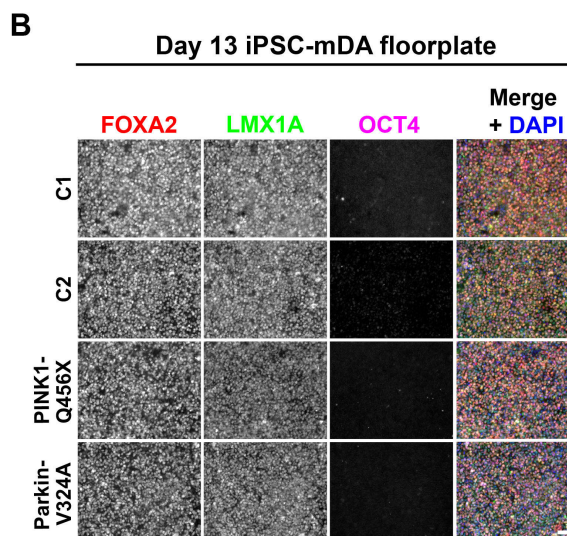
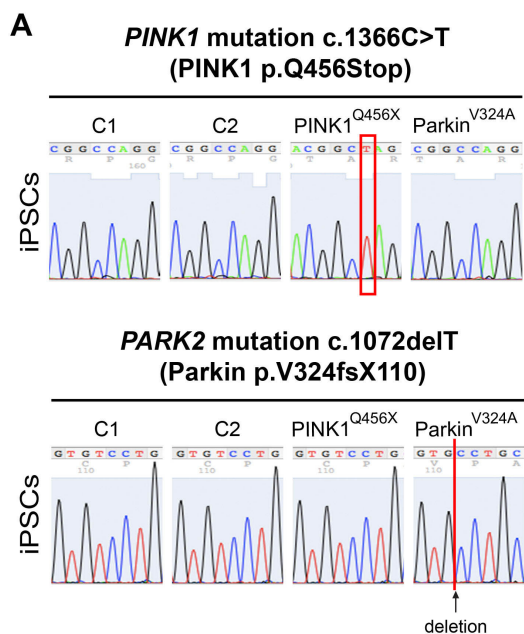


Figure S5. Differentiation of PD Mutant iPSCs into mDA Neurons and Characterization of Additional PD Patients, Related to Figure 6

(A) Sequencing for the homozygous *PINK1* c.1366C>T and *PARK2* c.1072delT mutations found in the PD mutant iPSCs but not in apparently healthy control iPSCs.

(B) Immunocytochemistry at day 13 of differentiation demonstrated no differences between healthy donors and PD patients in the conversion of OCT4+ iPSCs to FOXA2+/LMX1A+ mDA floorplate precursors.

(C) Further differentiation of precursors to post-mitotic mDA neurons was unaffected in PD mutant cells. *n*= at least 3 independent differentiations.

(D) Western blot analysis of AKT pathway signaling. Blots represent results from a replicate experiment of Figure 6F.

(E) Western blot analysis of AKT pathway signaling in an additional PD patient with a heterozygous mutation in Parkin (p.R275W). Numbers below the blots indicate the ratio of p-AKT (GFP-progerin) to p-AKT (nuclear-GFP). n, nuclear-GFP; p, GFP-progerin.

n.s. not significant, **p*<0.05 according to Student's t tests. Bar graph represents mean ± SEM.

Scale bars: 50 μm.

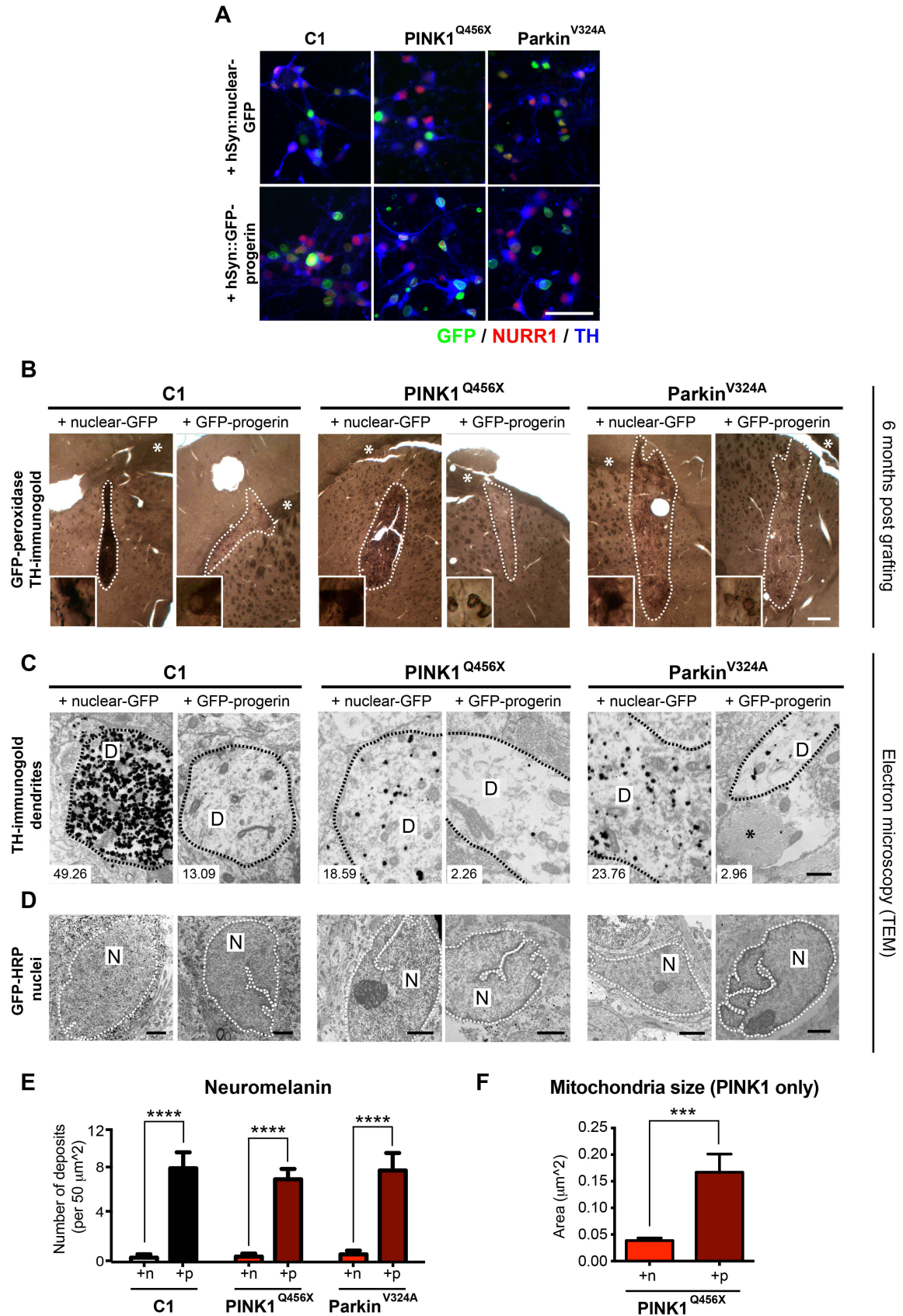


Figure S6. Characterization of Xenografts, Related to Figure 7

(A) Immunocytochemistry for NURR1 and TH in iPSC-mDA neurons replated *in vitro* and fixed 1-day post transplant. At least 50% of cells already expressed the synapsin-driven transgene at this timepoint.

(B) Immunohistochemistry for TH and GFP at 6 months post transplant demonstrates a dramatic loss of TH+ PD iPSC-derived mDA neurons when progerin is overexpressed. This pattern of TH loss in controls and PD mutants is similar to what was observed at 3 months post transplant (see Figure 7). Dotted line defines the graft. Asterisks denote the corpus callosum. Insets show a representative GFP+ nucleus.

(C and D) Ultrastructural analysis by transmission electron microscopy (EM). Representative (C) TH+ dendrites and (D) GFP+ nuclei are outlined and each labeled with a D or N, respectively. Number at bottom left represents the average number of TH-immunogold particles per μm^2 . Asterisk identifies a fibrillar body.

(E) Quantification of neuromelanin deposits from EM analysis. Ten $50 \mu\text{m}^2$ regions were analyzed per animal.

(F) Quantification of the area of 25 mitochondria in PINK1-Q456X animals from EM analysis.

*** $p < 0.001$ **** $p < 0.0001$ according to Student's t tests. Bar graphs represent mean \pm SEM.

Scale bars: $50 \mu\text{m}$ (A), $400 \mu\text{m}$ (B), 500 nm (C), $2 \mu\text{m}$ (D).

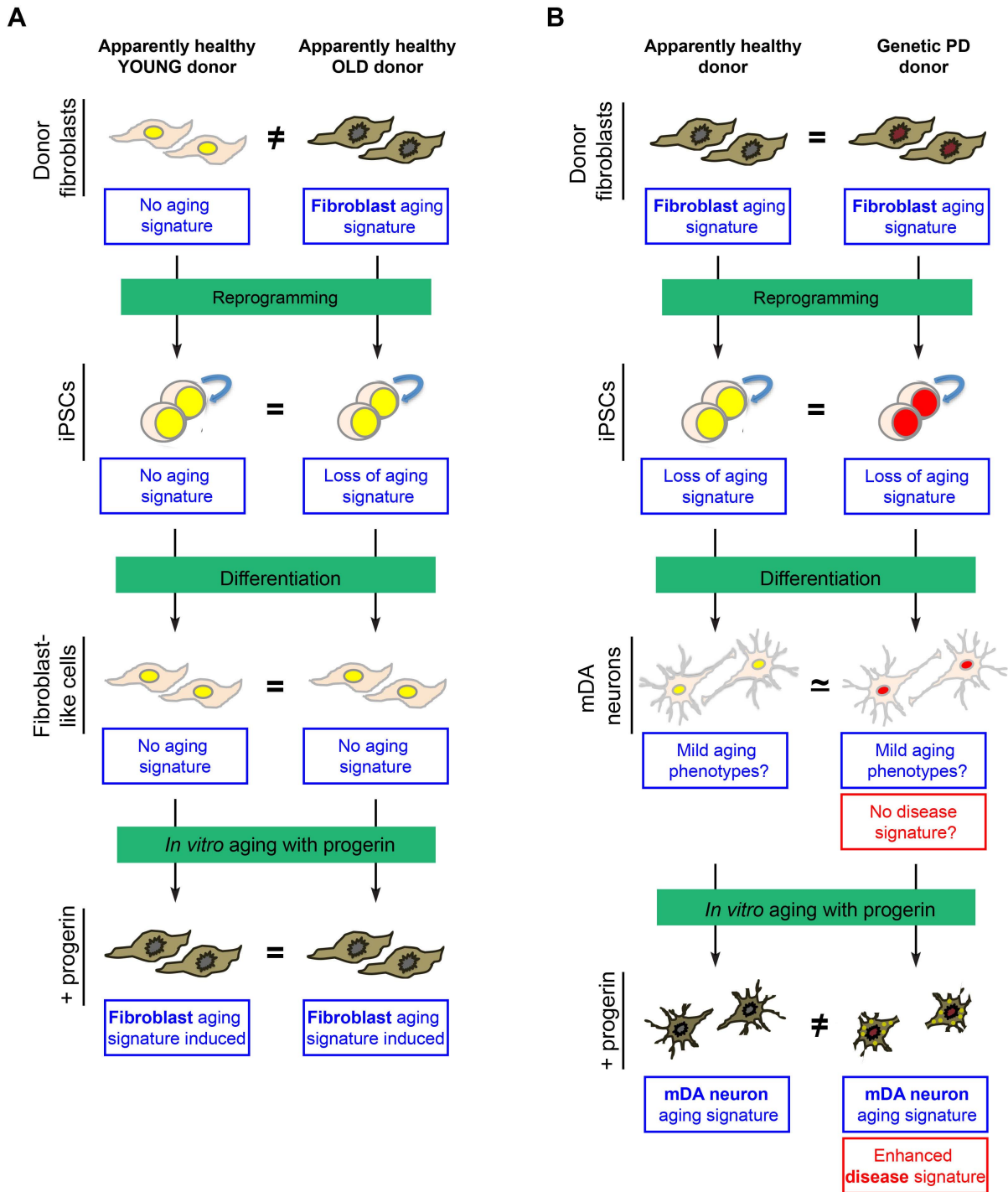


Figure S7. Summary Diagram, Related to Figures 1-7

(A) A set of age-associated markers found in primary fibroblasts derived from old donors are lost during reprogramming to iPSCs and are not regained upon differentiation of iPSCs to

fibroblast-like cells or mDA neurons. As a result, the reprogramming/differentiation paradigm generates cells with a “young” phenotype regardless of donor age. However, age-associated markers can be reestablished upon overexpression of progerin, giving rise to “old” iPSC-derived cells.

(B) iPSCs derived from PD patients and apparently healthy donors appear to be phenotypically identical despite their genotypic differences. Upon differentiation into mDA neurons only minor differences are observed between PD versus control cells (no/mild disease signature). However, progerin overexpression triggers an mDA aging-like signature and reveals multiple disease-associated phenotypes that require the interaction between genotype and phenotype in PD iPSC-derived mDA neurons (enhanced disease signature).

Table S1. Fibroblast Panel from Donors of Various Ages, Related to Figure 1

Mutation status	Age	Coriell reference number
Apparently healthy	11	GM01652
Apparently healthy	11	GM02036
Apparently healthy	11	GM01864
Apparently healthy	31	AG16146
Apparently healthy	40	GM02153
Apparently healthy	55	GM00967
Apparently healthy	71	GM01680
Apparently healthy	81	GM04204
Apparently healthy	82	GM01706
HGPS (c.1824C>T)	3	AG06917
HGPS (c.1824C>T)	8	AG06297
HGPS (c.1824C>T)	14	AG11498

Table S2. Summary of Phenotypes and Their Associated Markers, Related to Figures 1-7

Fibroblast aging signature	
Nuclear folding and blebbing	Lamin A/C
Loss of nuclear organization proteins	LAP2 α
Loss of heterochromatin	H3K9me3, HP1 γ
Accumulation of DNA damage	γ H2AX
Increased mitochondrial ROS generation	MitoSOX
Telomere shortening	Telomeric repeats Q-FISH probe
Upregulation of senescence markers	SA- β -Gal
mDA neuron aging signature	
Enhanced nuclear folding and blebbing	Lamin A/C
Accumulation of DNA damage	γ H2AX
Increased mitochondrial ROS generation	MitoSOX
Dendrite shortening	MAP2ab
Neurodegeneration gene expression signature	RNA-seq
Hyperactivation of p-AKT	p-AKT, p-4EBP1, p-ULK1
Mild decrease of TH+ neurons	TH <i>in vivo</i>
Accumulation of neuromelanin	Electron microscopy <i>in vivo</i>
PD disease signature	
Enhanced susceptibility to cell death activation	Cleaved caspase-3
Accelerated dendrite shortening	MAP2ab
Loss of p-AKT	p-AKT, p-4EBP1, p-ULK1
Pronounced/progressive loss of TH+ neurons	TH <i>in vivo</i>
Enlarged mitochondria	Electron microscopy <i>in vivo</i> – PINK1 only
Multilamellar inclusions	Electron microscopy <i>in vivo</i> – Parkin only

Table S3. Differentially Expressed Transcripts Following Progerin Overexpression in iPSC-mDA Neurons, Related to Figure 5

List of transcripts that were significantly differentially expressed (fold change +/- 2, $p < 0.05$) in both young and old donor-derived iPSC-mDA neurons between GFP-progerin and nuclear-GFP (nGFP) treatments.

Table S4. Antibodies Used for Molecular Analyses, Related to Figures 1-7

EM, electron microscopy; FC, flow cytometry; ICC, immunocytochemistry; IHC, immunohistochemistry; WB, western blot.

Antigen	Company	Host	Concentration
p-4EBP1	Cell Signaling	Rabbit	1:1000 (WB)
4EBP1 (total)	Cell Signaling	Rabbit	1:1000 (WB)
p-AKT	Cell Signaling	Rabbit	1:250 (WB)
AKT (total)	Cell Signaling	Rabbit	1:1000 (WB)
CD13-PE	BD		20 ul per 1 M cells (FC)
Cleaved caspase-3	Cell Signaling	Rabbit	1:100 (ICC)
FOXA2	Santa Cruz	Goat	1:200 (ICC)
GFP	Abcam	Chick	1:2000 (WB, IHC)
GFP	Aves	Chick	1:3000 (EM)
γ H2AX	Millipore	Mouse	1:250 (ICC)
H3K9me3	Abcam	Rabbit	1:4000 (ICC)
HLA-ABC-APC	BD		20 ul per 1 M cells (FC)
HP1 γ	Millipore	Mouse	1:200 (ICC)
Ki67	Dako	Mouse	1:100 (ICC)
Lamin A	Abcam	Rabbit	1:100 (ICC)
Lamin A/C (clone JOL2)	Abcam	Mouse	1:200 (ICC)
Lamin A/C (clone N-18)	Santa Cruz	Goat	1:100 (WB)
Lamin B2	Abcam	Mouse	1:500 (ICC)
Lamin C	Abcam	Rabbit	1:100 (ICC)
LAP2 α	Abcam	Rabbit	1:500 (ICC)
LMX1A	Millipore	Rabbit	1:2000 (ICC)
MAP2	Sigma	Mouse	1:200 (ICC)
NANOG	R&D	Goat	1:50 (ICC)
Nestin	R&D	Mouse	1:300 (ICC)
NURR1	R&D	Mouse	1:1000 (ICC)
OCT4	Santa Cruz	Mouse	1:200 (ICC)
Sendai	MBL Int.	Rabbit	1:500 (ICC)
SSEA3-FITC	BD		20 ul per 1 M cells (FC)
SSEA4-PE	BD		20 ul per 1 M cells (FC)
Total AKT	Cell Signaling	Rabbit	1:500 (WB)
TUJ1	Covance	Mouse/Rabbit	1:500 (ICC)
Tyrosine hydroxylase (TH)	Pel-Freez	Rabbit	1:500 (ICC, IHC, WB)

TH	Immunostar	Mouse	1:2000 (EM)
p-ULK1	Cell Signaling	Rabbit	1:500 (WB)
ULK1 (total)	Cell Signaling	Rabbit	1:1000 (WB)
Vimentin-Cy3	Sigma		1:200 (ICC)

Table S5. Sequences of Primers Used for Sequencing, PCR Analysis and RNA Generation, Related to Figures 1 and 3-7

Name	Application	Sequence (5' → 3')	Reference
cyclophilin A	qRT-PCR (SYBR)	F: GTCAACCCCACCGTGTTCTT R: CTGCTGTCTTTGGGACCTTGT	
GFP-progerin ORF	Modified RNA cloning	F: P-TGGTGAGCAAGGGCGCCGAGCTG R: P-TTACATGATGCTGCAGTTCTG	
lamin A	qRT-PCR (SYBR)	F: GCTCTTCTGCCTCCAGTGTC R: ACATGATGCTGCAGTTCTGG	
lamin C	qRT-PCR (SYBR)	F: CTCAGTGACTGTGGTTGAGGA R: AGTGCAGGCTCGGCCTC	
LMNA	Mutation sequencing	F: CTGAGCCTTGTCTCCCTTCC R: none	
LMNA exons 9-12	RT-PCR	F: GTGGAAGGCACAGAACACCT R: GTGAGGAGGACGCAGGAA	(Scaffidi and Misteli, 2006)
nuclear-GFP ORF	Modified RNA cloning	F: P-TGGTGAGCAAGGGCGCCGAGCTG R: P-TTATCTAGATCCGGTGGATCCTACC	
Parkin (c.1366C>T)	Mutation sequencing	F: GAAACTGGTTAAGCAAGAAATCC R: none	
PINK1 (c.1072delT)	Mutation sequencing	F: TGTGCAGGACATGAAAAGGT R: none	
progerin	qRT-PCR (SYBR)	F: GCGTCAGGAGCCCTGAGC R: GACGCAGGAAGCCTCCAC	
progerin ORF	Cloning into pAcGFP1-C	F: aaggcctctgtcgacAGCAGTCTCTGTCCTTC GACCC R: agaattcgcaagcttCTTCCACCTCCCACCTC ATTCC	
Tail PCR	Modified RNA cloning	F: TTGGACCCTCGTACAGAAGCTAATACG R: (Tx120)CTTCCTACTCAGGCTTTATTCAA AGACCA	(Warren et al., 2010)

SUPPLEMENTAL EXPERIMENTAL PROCEDURES

Generation and Characterization of iPSCs

Fibroblasts were purchased from Coriell (Camden, NJ) and reprogrammed based on a protocol modified from Fusaki et al. (Fusaki et al., 2009) using CytoTune Sendai viruses expressing OCT4, SOX2, KLF4, and c-MYC (OSKM; Life Technologies, Carlsbad, CA). Briefly, fibroblasts were plated onto gelatin at 10,500 cells per cm² per well of a 12-well plate in Minimal Essential Medium Alpha (Life Technologies) supplemented with 15% fetal bovine serum (Life Technologies). CytoTune viruses were combined at an MOI of 10 and added to the fibroblasts on the following day (notated as day 0) as well as on day 2 in some cases. Medium was replaced approximately 16 hours after addition. On day 4 fibroblasts were harvested by trypsinization and reseeded at 10,500 cells per cm² onto mitomycin C-treated mouse embryonic fibroblasts (MEFs; Global Stem, Rockville, MD) in iPSC maintenance medium containing DMEM-F12, 20% knockout serum replacement (Life Technologies), L-glutamine, non-essential amino acids, β -mercaptoethanol, and 10 ng/ml FGF2 (R&D) supplemented with 10 μ M Rho-kinase inhibitor (Y-27632; Tocris, Bristol, UK) to support attachment. The medium was replaced every other day thereafter. Valproic acid (Sigma, St Louis, MO) was added to the medium at a final concentration of 1 mM from day 6 to day 13 to enhance the reprogramming efficiency as described previously (Huangfu et al., 2008). In addition, the cells were cultured in 5% oxygen from 1 week prior to transduction through 2.5 weeks after transduction to further improve the likelihood of iPSC colony formation (Yoshida et al., 2009). HGPS fibroblasts were also treated with rapamycin (Sigma) at 680 nM from 1 week prior to transduction until the first appearance of iPSC colonies in order to reduce HGPS phenotypes (Cao et al., 2011), which can act as a barrier to reprogramming. Approximately 30 days after transduction, colonies resembling human embryonic stem cell colonies were mechanically isolated and replated onto MEFs in 24-well plates. iPSC clones were picked from separately transduced wells in order to ensure independent reprogramming events. At least 3 surviving colonies from each starting fibroblast line were subsequently maintained on MEF feeder layers in iPSC medium and passaged approximately every week using dispase (STEMCELL Technologies, Vancouver, BC). Karyotype analysis was performed by the MSKCC Molecular Cytogenetics core facility using standard G-banding procedures. Spontaneous differentiation via embryoid body formation was performed as described previously (Park et al., 2008). Experiments using iPSCs were performed using 3 independent clones per fibroblast line. All cells (including those listed below) were regularly tested for mycoplasma every 2 to 4 weeks and found to be negative.

iPSCs for PD Modeling

PD iPSCs generated by retroviral overexpression of OSKM from patients with mutations in PINK1 (c.1366C>T, p.Q456XStop) or PARK2/Parkin (c.1072Tdel, p.V324fsX110) were generously provided by the D. Krainc lab (Massachusetts General Hospital, Boston, MA). Apparently healthy iPSCs (C1, age 36; C2, age 48) also established using pMIG retroviruses (OSK, no c-Myc) were obtained from the K. Eggan lab (Harvard University, Cambridge, MA). Additional iPSC clones were derived using Sendai virus from fibroblasts from a patient with a different mutation in PARK2/Parkin (c.924C>T, p.R275W). Young (here called C3) and old

(here called C4) iPSCs listed above were used as controls because they were also derived using Sendai virus reprogramming factors.

Fibroblast Differentiation

Differentiation of iPSCs to fibroblast-like cells was based on a protocol from Park et al. (Park et al., 2008). Briefly, iPSC clones were enzymatically passaged using dispase and plated as multi-cell clumps onto gelatin in iPSC maintenance medium that had been conditioned on MEFs for 24 hours and then supplemented with 10 ng/ml FGF2 and 10 μ M Y-27632. The next day the medium was replaced with Minimal Essential Medium Alpha (Life Technologies) supplemented with 15% fetal bovine serum (Life Technologies) and continually changed every other day thereafter. The differentiating cells were carefully passaged every 5-6 days using Accutase (Innovative Cell Technology, San Diego, CA) for the first two weeks and then trypsinized subsequently. Y-27632 was added to the medium on the day of passaging to help support attachment. After four weeks fibroblast-like cells were sorted based on high expression levels of CD-13 and HLA-ABC prior to phenotype assessment and overexpression studies. Sorted cells were expanded in Minimal Essential Medium Alpha with 15% fetal bovine serum (no Y-27632) thereafter.

mDA Neuron Differentiation

A modified version of the dual-SMAD inhibition protocol was used to direct cells towards floor plate-based mDA neurons as described previously (Kriks et al., 2011) and schematized in **Figure S3A**. iPSC-derived mDA neurons were replated on day 30 of differentiation at 260,000 cells per cm^2 on dishes pre-coated with polyornithine (PO; 15 μ g/ml)/ Laminin (1 μ g/ml)/ Fibronectin (2 μ g/ml) in Neurobasal/B27/L-glutamine-containing medium (NB/B27; Life Technologies) supplemented with 10 μ M Y-27632 (until day 32) and with BDNF (brain-derived neurotrophic factor, 20 ng/ml; R&D), ascorbic acid (AA; 0.2 mM, Sigma), GDNF (glial cell line-derived neurotrophic factor, 20 ng/ml; R&D), TGF β 3 (transforming growth factor type β 3, 1 ng/ml; R&D), dibutyryl cAMP (0.5 mM; Sigma), and DAPT (10 nM; Tocris,). One to two days after plating, cells were treated with 1 μ g/ml mitomycin C (Tocris) for 1 hour to kill any remaining proliferating contaminants. iPSC-derived mDA neurons were fed every 2 to 3 days and maintained without passaging until the desired timepoint for a given experiment. PO, laminin and fibronectin were added to the medium every 7-10 days to prevent neurons from lifting off.

Synthetic mRNA (Modified-RNA) Cloning, Synthesis and Use

Modified-RNA was generated using an *in vitro* transcription (IVT) protocol described previously (Mandal and Rossi, 2013; Warren et al., 2010). The ORF for progerin was obtained by PCR from HGPS fibroblasts. N-terminal GFP fusion was achieved by inserting the progerin ORF into pAcGFP1-C using InFusion® cloning technology (Clontech, Mountain View, CA). Nuclear GFP was templated from pAcGFP1-Nuc (Clontech). Phosphorylated ORFs were cloned into a backbone already containing generic 5' and 3' UTRs (provided by the D. Rossi lab; Harvard Medical School, Boston, MA). Tail PCR and IVT reactions were carried out as described previously (Mandal and Rossi, 2013). For overexpression experiments, modified-RNA was thawed on ice and adjusted to a working concentration of 100ng/ μ l. Modified-RNA and Lipofectamine RNAiMAX® (Life Technologies, 1 μ g modified RNA:3 μ l Lipofectamine) were

initially prepared in Opti-MEM separately, gently mixed and incubated at room temperature for 10 minutes. The Lipofectamine mixture was then transferred to the tube containing the modified-RNA mixture, gently mixed and incubated for an additional 10 minutes. 1 µg of modified-RNA was added per 80,000 fibroblasts in a single 24-well. 200 ng of modified-RNA was added per 100,000 neurons in a single 96-well. The transfection mixture was added dropwise to cells that had been pre-treated with 200 ng/ml of the interferon inhibitor B18R (eBioscience, San Diego, CA) for at least 4 hours prior to transfection. After 4 hours at 37°C, the entire suspension was replaced with fresh medium supplemented with B18R. Transfection of iPSC-derived fibroblasts was performed starting on day 50 of differentiation and repeated on 2 consecutive days thereafter. iPSC-derived mDA neurons were transfected starting on day 65 or day 120 of differentiation and repeated on 4 consecutive days thereafter. The additional 2 days of transfections were required in order to establish a progerin expression levels equivalent to the iPSC-derived fibroblasts. All cells were analyzed one day after the final transfection.

Immunostaining

Cells

Cells were fixed in 4% paraformaldehyde for 15 minutes. Blocking was performed in phosphate-buffered saline supplemented with 1% BSA, and 0.3% Triton X-100 for 30 minutes to 1 hour. Cells were stained overnight at 4°C with primary antibodies diluted in blocking buffer. A list of antibodies and concentrations is provided in **Table S4**. Following several washes, cells were stained with appropriate Alexa Fluor-labeled secondary antibodies (Molecular Probes, Carlsbad, CA) at 1:500 in blocking buffer for 30 minutes to 3 hours at room temperature. Cells were counterstained with 4',6-diamidino-2-phenylindole (DAPI; Thermo Fisher, Rockford, IL) to visualize nuclei. Images were acquired with an Olympus IX81 microscope using a Hamamatsu ORCA CCD camera.

Mouse Tissue

3 months after transplantation of human iPSC-derived mDA neurons, mice received overdoses of Pentobarbital intraperitoneally (50 mg/kg) to induce deep anesthesia and were perfused in 4% paraformaldehyde (PFA). Brains were extracted, post-fixed in 4% PFA then soaked in 30% sucrose solutions for 2-5 days. The tissue was sectioned (30 µm) on a cryostat after embedding in O.C.T. (Sakura-Finetek, Torrance, CA). For treatment of mouse tissue for electron microscopy, see below.

Immunostaining Quantification

In Vitro Cells

Images were acquired on an Operetta (PerkinElmer, Waltham, MA) using a 20X objective. Image processing was performed using Harmony high content analysis software (version 3.0). Passage-matched cells were scored from three independent experiments. Where necessary due to bias against progerin-positive cells, images were processed using ImageJ software (version 1.43u, NIH). In these cases, 50 cells per condition were assessed for each independent experiment. All data are presented as mean ± standard error of means (SEM).

In Vivo Mouse Brain Tissue

Cell counts were determined using the optical fractionator probe and the Cavalieri estimator using the Stereo Investigator software (MBF bioscience, Vermont) as described previously

(Tabar et al., 2005). Cell counts were scored on every fifth section where a graft was identifiable using a randomized grid. Counts were determined from three animals per condition (J.D.M. was not blinded to experimental groups). Data are presented as estimated total cell number \pm SEM.

Assessment of Senescence

Senescence-activated beta-galactosidase was assessed using the staining kit from Cell Signaling according to the manufacturer's instructions. Positive cell staining was manually assessed (2 replicates, 50 cells each).

Telomere Length Measurements by HT-QFISH

Cells were plated on a clear-bottom, black-walled, 96-well plate, including 4 well replicates per sample, and high throughput quantitative fluorescence in situ hybridization (HT-QFISH) was performed as previously described (Canela et al., 2007). Images were captured with the Operetta using a 20X objective. Image processing was performed using Harmony high content analysis software. Telomere length values were measured using individual telomere spots corresponding to the specific binding of a Cy3-labeled telomeric probe (>600 spots per sample) in quadruplicate samples, fluorescence intensities were converted into kilobases using control cell lines of known telomere length as described previously (Canela et al., 2007; McIlrath et al., 2001).

Flow Cytometry

Cells were dissociated with Accutase and stained with directly conjugated antibodies (BD Biosciences, San Jose, CA) according to manufacturer-recommended concentrations for 1 hour on ice. Cell sorting was performed on a FACSAria (BD Biosciences).

Mitochondrial ROS Assessment

Cells were dissociated with Accutase and stained with MitoSOX Red mitochondrial superoxide indicator (Life Technologies) at a final concentration of 20 μ M in cell culture medium. Staining was carried out in a 37°C incubator for 30 minutes. Cells were washed and resuspended in cell culture medium containing DAPI to exclude dead cells from the analysis. In order to prevent positive staining due to cell shock, all reagents used were pre-warmed to 37°C and samples were kept at 37°C until just prior to analysis on a FACSAria. Samples were always compared to untreated young donor fibroblasts/iPSC-derived fibroblasts/iPSC-derived mDA neurons as well as the young donor cells treated with 20 μ M carbonyl cyanide 3-chlorophenylhydrazone (CCCP; Sigma) for 48 hours to induce mitochondrial superoxide production. These controls helped to ensure that the reagent had not become oxidized over time and that the cells were not stressed during the staining protocol. Quantification of the percent of the population that oxidized the MitoSOX reagent was performed using FlowJo software (version 9.5.3; Tree Star) and averaged for at least three independent clones or experiments per condition. All data from an individual experiment were excluded from analysis when the negative control sample gave an entirely positive reading by flow cytometry, suggesting that the conditions or the reagent itself were compromised.

DNA Extraction and Mutation Analysis

Genomic DNA was extracted from cell pellets using the DNeasy blood and tissue kit (Qiagen). A small region around the mutation was PCR amplified using HiFi Hotstart (KAPA Biosystems) per the manufacturer's instructions (for primers used see **Table S5**). PCR products were cleaned up using standard phenol/chloroform extraction and ethanol precipitation. DNA sequencing of PCR products was performed by the MSKCC DNA Sequencing core facility or GENEWIZ (South Plainfield, NJ).

RNA Extraction and Gene Expression Analysis

Cells were lysed directly in Trizol (Life Technologies). RNA was extracted using chloroform and ethanol precipitation and further cleaned using the RNeasy kit (Qiagen). Samples were stored at -80°C until further processing. Total RNA was reverse transcribed (Superscript, Life Technologies) and 50 ng of RNA was used to template each RT-PCR reaction. For analysis of progerin expression levels, total RNA was hydrolyzed by 0.1X volume 5 M NaOH for 30 minutes at room temperature followed by 0.1X volume 5 M HCl (Scaffidi and Misteli, 2006). Quantitative RT-PCR was performed using the Mastercycler RealPlex2 (Eppendorf, Hauppauge, NY) platform following the manufacturer's instructions. Expression levels were normalized to cyclophilin A or 18S (housekeeping gene controls) as noted. For RNA-seq, total RNA was isolated from two independent experiments and processed by the MSKCC Genomic core facility. Paired-end 75 base pair RNA-sequencing libraries were sequenced on an Illumina HiSeq2000. Reads were mapped to the human genome (Hg19) using STAR 2.3.0e (Dobin et al., 2013) with default mapping parameters and read counts were assessed using HTSeq. Principal component analysis was completed in R (v2.15.2) using the base "stats" package. Differentially expressed genes were identified with limma voom (Smyth, 2004). A conservative approach was taken to account for low coverage in the sequencing library; a low read count filter was used such that all samples must contain non-zero read counts for a gene to be assessed in limma. Differentially expressed genes were identified using a fold change cut off of +/- 2 and a Bonferroni adjusted p value of 0.05. A hypergeometric test was used to assess the similarity in response to progerin overexpression in young donor and old donor iPSC-derived mDA neurons. Gene ontology analysis was completed using iPAGE (Goodarzi et al., 2009) with the fold change between nuclear-GFP and GFP-progerin expressing iPSC-derived mDA neurons as a continuous variable across 10 bins. Venn-diagrams, barplots, and PCA plots were generated in R (v2.15.2) using the base R 'ggplot2' graphics packages (Wickham, 2009). Raw data are available on Gene expression omnibus <http://www.ncbi.nlm.nih.gov/geo/> (GSE49112).

Protein Isolation and Western Blot Analysis

Cells were collected with a cell lifter (Corning, Tewksbury, MA) in ice-cold phosphate-buffered saline without calcium or magnesium (PBS-/). Cell pellets were rapidly frozen on ethanol and dry ice and stored at -80°C. Cell pellets were thawed on ice and resuspended in 50-200 µl RIPA lysis buffer (50 mM Tris-HCl pH 8.0, 120 mM NaCl, 5 mM EDTA, 0.5% NP-40) with 1% sodium dodecyl sulfate (SDS). Cell suspensions were vortexed at 15-minute intervals during a 45-minute incubation on ice. Lysates were isolated following a 10,000 rpm spin for 10 minutes at 4°C. 20-40 µg samples were further diluted with 4X Laemmli sample buffer, boiled for 5

minutes at 95°C, and loaded onto a NuPAGE 4-12% Bis-Tris precast gel (Life Technologies). Gel electrophoresis was performed at 100 V for 2 hours. Gels were transferred to a methanol-activated PVDF membrane using the XCell II Blot Module (Life Technologies) according to the manufacturer's instructions. Blots were blocked in 3% bovine serum albumin (BSA) in Tris-buffered saline plus 0.1% Tween-20 (TBS-T) for 45 minutes at room temperature. Blots were incubated in primary antibodies overnight at 4°C on shaker (see **Table S4** for a list of antibodies used). Following several washes with TBS-T, blots were incubated in appropriate HRP-labeled secondary antibodies (Jackson ImmunoResearch, West Grove, PA) for 1 hour at room temperature. Visualization of protein bands was performed using Western Lightning Plus-ECL (PerkinElmer, Melville, NY) according to the manufacturer's instructions and developed on an SRX-101A x-ray film processor (Konica Minolta, Wayne, NJ). Densitometry quantification was performed using ImageJ on blots from three independent experiments.

Neurite Quantification

Following immunostaining with MAP2 to label dendrites, randomly chosen images of GFP+ cells were manually acquired on an Olympus IX81 microscope using a Hamamatsu ORCA CCD camera using a 40X objective. Dendrite lengths were measured using ImageJ to trace each labeled neurite extending from GFP+ nuclei (J.D.M. was not blinded to experimental groups). Cells with only perinuclear MAP2 staining were given a zero. GFP+ nuclei without MAP2 staining as well as cells with condensed GFP+ nuclei were not scored. Fifty cells per condition were assessed for each of three independent differentiations.

***In Vivo* Assessment**

Transplantation

Animal procedures were performed following NIH guidelines and were approved by the local Institutional Animal Care and Use Committee (IACUC), the Institutional Biosafety Committee (IBC) as well as the Embryonic Stem Cell Research Committee (ESCRO). Six-week-old *NOD-SCID IL2Rgc*-null mice (20–35 g; Jackson Laboratory, Bar Harbor, ME) were anesthetized with Ketamine (90 mg/kg; Akorn, Decatur, IL) and Xylazine (4 mg/kg Fort Dodge, IA). 10 µg 6-hydroxydopamine (6-OHDA (Sigma-Aldrich) was injected stereotactically into the striatum of 6-week-old mice at the following coordinates (in millimeters): AP, 0.5 (from bregma); ML, -2.0; DV, -3.0 (from dura). Two weeks after lesioning, mice were tested twice (1 week apart) for rotational behavior (see below). Animals were divided into six groups so that those demonstrating high/low rotations were evenly distributed among the groups and then randomly assigned to a particular group. Y.M.G. was blind to the naming of the experimental groups. An initial sample size of 5 animals per condition was chosen to allow for analysis of at least 3 animals per group at the 3-month timepoint. Control (C1) and PD mutant (PINK1-Q456X, Parkin-V324A) iPSC-derived mDA neurons were infected with lentiviral vectors expressing either *hSyn::GFP-progerin* or *hSyn::nuclear-GFP* on day 21 of differentiation and transplanted on day 30 (animals approximately 2.5-months-old at time of transplantation). A total of 200×10^3 cells were injected in a volume of 2 µl into the striatum at the following coordinates (in mm): AP, 0.5; ML, -1.8; DV, 3.2.

Rotation testing

Amphetamine-induced rotation testing was performed before transplantation and 12 after transplantation. Rotation behavior in mice was recorded 10 min after i.p. injection of d-amphetamine (10 mg/kg, Sigma) and recorded for 30 minutes. The data were presented as the average number of rotations per minute.

Electron Microscopy

All procedures were performed according to (Milner et al., 2011). Briefly, six months following transplantation of human iPSC-derived mDA neurons, mice were overdosed with 150 mg/kg sodium pentobarbital intraperitoneally. The brains were fixed by aortic arch perfusion sequentially with normal saline (0.9%) containing 1000 units /ml of Heparin, 50 ml of 3.75% acrolein and 2% paraformaldehyde in 0.1 M phosphate buffer (PB, pH 7.4), and 200 ml of 2% PFA in PB. The brains were removed and post-fixed with 1.87% acrolein/2% PFA in PB for 30 minutes at room temperature. Coronal tissue blocks were sectioned (40 μm) on a vibrating microtome (Leica Microsystems, Deerfield, IL). Selected sections containing the xenograft were pretreated in 1% sodium borohydride. Non-specific binding was blocked with 0.5% BSA 0.1 M Tris-saline (TS, pH 7.6). Primary antibodies (see **Table S4**) were diluted in 0.1% BSA in TS and incubated overnight at 4°C. Sections were incubated with a biotinylated secondary antibody (Jackson ImmunoResearch, West Grove, PA) for 30 minutes at room temperature. Peroxidase labeling was performed using the Vectastain ABC kit (Vector Laboratories, Burlingame, CA) followed by incubation with diaminobenzidine for 7 minutes. Sections were then incubated in gold-conjugated secondary antibody (Electron Microscopy Sciences (EMS), Fort Washington, PA) overnight at 4°C. Sections were post-fixed in 2% glutaraldehyde, washed in 0.2M citrate buffer (pH 7.4), and silver intensified using the Silver IntenSE M kit (GE Healthcare, Piscataway, NJ). Following several washes, sections were fixed in 2% osmium tetroxide for 1 hr, dehydrated through an ascending ethanol series, and placed in propylene oxide/EMBed 812 (EMS) overnight. Sections were then embedded in EMBED 812 between two sheets of Aclar plastic at 60°C for 4 days. Selected sections containing the graft were glued on Beem capsules and cut on an ultramicrotome (Ultracut) using a glass knife (Leica). Ultrathin sections were collected on grids and counterstained with uranyl acetate and Reynold's lead citrate. Final preparations were examined and photographed using a Phillips C10 transmission electron microscope. The number of TH-immunogold particles per μm^2 in 25 dendrites per group and the area (μm^2) quantification of 25 mitochondria per group were performed using ImageJ.

Statistical Analysis

Frequency distribution plots display the fluorescence intensity quantification of 100 cells (fibroblasts) or 50-100 cells from each of 3 independent experiments (all others) binned by 50 or 100 arbitrary unit increments. Distributions were compared by statistical analysis of corresponding cumulative distributions using Kolmogorov-Smirnov tests to analyze the difference between different ages or treatments. Arbitrary units for frequency distributions of different cell types should not be compared because staining was performed at different times. Bar graphs are plotted as mean \pm SEM and represent 3 biological replicates except where noted. Technical replicates were averaged prior to being included in statistical analysis (i.e. average of technical replicates for 1 experiment = 1 biological replicate). Two-group comparisons were analyzed using Student t-tests. Multiple group comparisons against a control

were analyzed using an ANOVA with Dunnett's test. Prism (version 6.0a, GraphPad) was used for data presentation and analysis.

SUPPLEMENTAL REFERENCES

Cao, K., Graziotto, J.J., Blair, C.D., Mazzulli, J.R., Erdos, M.R., Krainc, D., and Collins, F.S. (2011). Rapamycin reverses cellular phenotypes and enhances mutant protein clearance in Hutchinson-Gilford progeria syndrome cells. *Science translational medicine* 3, 89ra58.

Dobin, A., Davis, C.A., Schlesinger, F., Drenkow, J., Zaleski, C., Jha, S., Batut, P., Chaisson, M., and Gingeras, T.R. (2013). STAR: ultrafast universal RNA-seq aligner. *Bioinformatics* 29, 15-21.

Goodarzi, H., Elemento, O., and Tavazoie, S. (2009). Revealing global regulatory perturbations across human cancers. *Mol Cell* 36, 900-911.

Huangfu, D., Osafune, K., Maehr, R., Guo, W., Eijkelenboom, A., Chen, S., Muhlestein, W., and Melton, D.A. (2008). Induction of pluripotent stem cells from primary human fibroblasts with only Oct4 and Sox2. In *Nat Biotechnol*, pp. 1269-1275.

McIlrath, J., Bouffler, S.D., Samper, E., Cuthbert, A., Wojcik, A., Szumiel, I., Bryant, P.E., Riches, A.C., Thompson, A., Blasco, M.A., *et al.* (2001). Telomere length abnormalities in mammalian radiosensitive cells. *Cancer research* 61, 912-915.

Park, I.-H., Zhao, R., West, J.A., Yabuuchi, A., Huo, H., Ince, T.A., Lerou, P.H., Lensch, M.W., and Daley, G.Q. (2008). Reprogramming of human somatic cells to pluripotency with defined factors. In *Nature*, pp. 141-146.

Smyth, G.K. (2004). Linear models and empirical bayes methods for assessing differential expression in microarray experiments. *Statistical applications in genetics and molecular biology* 3, Article3.

Tabar, V., Panagiotakos, G., Greenberg, E.D., Chan, B.K., Sadelain, M., Gutin, P.H., and Studer, L. (2005). Migration and differentiation of neural precursors derived from human embryonic stem cells in the rat brain. In *Nat Biotechnol*, pp. 601-606.

Wickham, H. (2009). *ggplot2: elegant graphics for data analysis* (Springer New York).

Yoshida, Y., Takahashi, K., Okita, K., Ichisaka, T., and Yamanaka, S. (2009). Hypoxia enhances the generation of induced pluripotent stem cells. In *Cell Stem Cell*, pp. 237-241.